Mwakal Alin

dr

Quick Submit

Quick Submit

Sokoine University of Agriculture

Document Details

Submission ID

trn:oid:::1:3278681742

Submission Date

Jun 17, 2025, 11:36 AM GMT+4

Download Date

Jun 17, 2025, 11:39 AM GMT+4

File Name

RECENT_PAPER_1_new_to_be_submitted_R4new.docx

File Size

6.4 MB

30 Pages

6,723 Words

39,165 Characters

18% Overall Similarity

The combined total of all matches, including overlapping sources, for each database.

Match Groups

- **122** Not Cited or Quoted 17%
  Matches with neither in-text citation nor quotation marks
- **1** Missing Quotations 0%
  Matches that are still very similar to source material
- **0** Missing Citation 0%
  Matches that have quotation marks, but no in-text citation
- **0** Cited and Quoted 0%
  Matches with in-text citation present, but no quotation marks

Top Sources

18% Internet sources
0% Publications
0% Submitted works (Student Papers)

Integrity Flags

0 Integrity Flags for Review

No suspicious text manipulations found.

Our system's algorithms look deeply at a document for any inconsistencies that would set it apart from a normal submission. If we notice something strange, we flag it for you to review.

A Flag is not necessarily an indicator of a problem. However, we'd recommend you focus your attention there for further review.

Match Groups

- **122** Not Cited or Quoted 17%
  Matches with neither in-text citation nor quotation marks
- **1** Missing Quotations 0%
  Matches that are still very similar to source material
- **0** Missing Citation 0%
  Matches that have quotation marks, but no in-text citation
- **0** Cited and Quoted 0%
  Matches with in-text citation present, but no quotation marks

Top Sources

18% Internet sources
0% Publications
0% Submitted works (Student Papers)

Top Sources

The sources with the highest number of matches within the submission. Overlapping sources will not be displayed.

1	Internet	www.mdpi.com 1%
2	Internet	www.tandfonline.com <1%
3	Internet	www.researchsquare.com <1%
4	Internet	www.frontiersin.org <1%
5	Internet	www.science.gov <1%
6	Internet	univendspace.univen.ac.za <1%
7	Internet	phd-dissertations.unizik.edu.ng <1%
8	Internet	studylib.es <1%
9	Internet	sistema.atenaeditora.com.br <1%
10	Internet	mdpi-res.com <1%

11	Internet	
www.degruyter.com		<1%
12	Internet	
www2.mdpi.com		<1%
13	Internet	
www.medrc.org		<1%
14	Internet	
asianpubs.org		<1%
15	Internet	
coek.info		<1%
16	Internet	
www.researchgate.net		<1%
17	Internet	
prr.hec.gov.pk		<1%
18	Internet	
repository.biust.ac.bw		<1%
19	Internet	
repository.mines.edu		<1%
20	Internet	
c.coek.info		<1%
21	Internet	
repository.lib.ncsu.edu		<1%
22	Internet	
core.ac.uk		<1%
23	Internet	
ftp.academicjournals.org		<1%
24	Internet	
www.seu.ac.lk		<1%

25 Internet
iasks.org <1%

26 Internet
studylib.net <1%

27 Internet
umu.diva-portal.org <1%

28 Internet
acikbilim.yok.gov.tr <1%

29 Internet
depot.ceon.pl <1%

30 Internet
m.moam.info <1%

31 Internet
mobt3ath.com <1%

32 Internet
pubs.rsc.org <1%

33 Internet
scielo.org.za <1%

34 Internet
link.springer.com <1%

35 Internet
scholar.sun.ac.za <1%

36 Internet
www.ukm.my <1%

37 Internet
banglajol.info <1%

38 Internet
ijlsci.in <1%

39	Internet	
www.ijtsrd.com		<1%
40	Internet	
www.ingentaconnect.com		<1%
41	Internet	
assets-eu.researchsquare.com		<1%
42	Internet	
ceenve.ceng.calpoly.edu		<1%
43	Internet	
rke.abertay.ac.uk		<1%
44	Internet	
www.nepjol.info		<1%
45	Internet	
dr.ntu.edu.sg		<1%
46	Internet	
healthfact.in		<1%
47	Internet	
ijer.ut.ac.ir		<1%
48	Internet	
pdffox.com		<1%
49	Internet	
repositorio.unesp.br		<1%
50	Internet	
repository.up.ac.za		<1%
51	Internet	
www.scielo.br		<1%
52	Internet	
eacademic.ju.edu.jo		<1%

53 Internet
eprints.kfupm.edu.sa <1%

54 Internet
www.jgenng.com <1%

55 Internet
7e5f9f31-6e38-498e-ace9-ed3e34bb48c4.filesusr.com <1%

56 Internet
arcabc.ca <1%

57 Internet
corpus.ulaval.ca <1%

58 Internet
es.tjfyhxt.com <1%

59 Internet
ethesis.nitrkl.ac.in <1%

60 Internet
ir.lib.uwo.ca <1%

61 Internet
journalrepository.org <1%

62 Internet
jrtppi.id <1%

63 Internet
lutpub.lut.fi <1%

64 Internet
mafiadoc.com <1%

65 Internet
medjchem-v3.azurewebsites.net <1%

66 Internet
opus.lib.uts.edu.au <1%

67 Internet

vixra.org <1%

68 Internet

www.preprints.org <1%

69 Internet

www.sciencedirect.com <1%

Efficient and Reusable Activated Carbon from *Aframomum angustifolium* Shells for Removal of Ceftriaxone from Aqueous Solution; Adsorption Isotherms, Kinetics, and Thermodynamic Studies

Baraka Kasazi [a], Alinanuswe Mwakalesi [a*], and Emmy Lema [a'].

[a]Department of Chemistry and Physics, College of Natural and Applied Sciences, Sokoine University of Agriculture, P.O. Box 3038, Morogoro, Tanzania.

Corresponding author: Tel.: +255 742722318

E-mail address: mwakalesi@sua.ac.tz.

ABSTRACT

The accumulation of antibiotics such as ceftriaxone in aquatic systems is a growing global concern due to their potential risks to human and ecological health. The removal of ceftriaxone from aqueous solutions using activated carbon from *Aframomum angustifolium* shells (biowaste) is reported. The activated carbon was characterized using BET, FTIR and SEM-EDAX. The fabricated activated carbon showed a high surface area of 1895.6 m²/g that allowed its reuse for five consecutive cycles without active site regeneration. Ceftriaxone removal efficiency was influenced by pH, temperature, and initial concentration. Optimal removal efficiency (97.8%) was achieved at pH 2, 298.15 K, and 200 mg/L ceftriaxone. The adsorption process followed both Langmuir (R^2 = 0.9862) and Freundlich (R^2 = 0.9833) isotherms, and kinetics fitted the Pseudo-Second-Order model. The adsorption was spontaneous (ΔG = – 6.80 kJ/mol) and exothermic (ΔH = – 4.43 kJ/mol), with increased randomness at the solid-solution interface (ΔS = 7.69 J/mol·K). The adsorbent displayed high efficiencies for the removal of ceftriaxone from real water samples of distilled water (97.47%), river water (98.61%) and well water (97.15%). The findings from the current study suggest the adsorbent material from the bio-waste is a promising, low-cost adsorbent for removing ceftriaxone and related contaminants from aqueous environment.

Keywords: *Aframomum angustifolium*, biowaste, activated carbon, ceftriaxone, antibiotic

1.0 INTRODUCTION

Pharmaceutical compounds are regarded as emerging environmental pollutants due to their high availability and widespread uses. Antibiotics are estimated to account 16.3% of the total medicine consumption [1]. Some antibiotics are indeed degraded in the body while others are excreted unchanged [2]. Consequently, the increasing prevalence of antibiotic residues in aqueous environments has raised significant concerns due to their potential adverse effects on ecosystems and human health [3]. Health problems associated with the accumulation of antibiotics in the environment include cancer, neurotoxicity, mental disorders, and impaired immune function [4]. The development of antibiotic resistance genes is also an emerging challenge linked to the accumulation of antibiotic residues in aquatic environments [5]. Cephalosporins are a class of widely used antibiotics due to their strong bactericidal action and broad antibacterial spectrum. Consequently, they are employed to treat various bacterial infections, including acute pneumonia, bone and joint infections, respiratory infections, urinary tract infections, soft tissue infections, skin infections, and bloodstream infections. However, the accumulation of cephalosporins in the environment is a growing concern due to their toxic effects on ecosystems, even at low doses [6]. Adverse effects reported in Dario rerio (zebrafish) exposed to cephalosporins include reduced body length, shortened yolk sac length and height, and DNA damage [7].

Different methods, including adsorption, chemical oxidation, photochemical degradation, ozonation, ion exchange, photocatalysis, and biological processes, have been developed to remove ceftriaxone from aqueous solutions [8]. However, most of these methods face challenges such as continuous chemical consumption, sludge generation, and high maintenance costs, while biological methods suffer from poor biodegradation efficiency for some antibiotics [8]. The adsorption method is the most preferred technique for the removal of ceftriaxone due to its effectiveness, cheapness and versatility

Activated carbon (AC) is a highly effective adsorbent for removing different contaminants due to its high surface area, porous structure, and versatile surface chemistry [9]. Traditionally, AC is produced from non-renewable sources like coal, which involves significant energy consumption, high costs, resource depletion, health and safety concerns, and environmental impacts such as land degradation, and greenhouse gas emissions from mining and processing [10, 11]. Therefore, interest is growing in developing AC from renewable and sustainable materials, particularly agricultural and forestry biowastes. These offer potentially more sustainable, environmentally friendly, and cost-effective solutions [12]. Utilizing biowastes also reduces greenhouse gas emissions associated with their decomposition upon disposal in landfills [13]. Most agricultural

products are rich in cellulose, hemicellulose, and lignin, making them suitable AC precursors due to their abundance of functional groups like hydroxyl, carboxylic, and phenolic groups [14]. These functional groups enhance AC's selectivity for various chemical contaminants through interactions [15].

A. angustifolium is a tropical plant in Africa bearing edible fruits consumed in countries like Tanzania, Uganda, and the Democratic Republic of Congo [16-18]. The fruit shells of *A. angustifolium* (FPAA) are discarded as biowaste. However, these shells are rich in cellulose, hemicellulose, and lignin, making them suitable for AC production [19]. Limited information exists on utilizing this waste for AC synthesis. This study therefore reports the synthesis and application of AC derived from FPAA for removing cephalosporin antibiotics, using ceftriaxone as a model compound, from aqueous environments. In the current study, we present a novel and sustainable method for removing this persistent antibiotic using AC derived from this biowaste. Transforming abundant agricultural waste into high-surface-area carbon valorizes a low-value byproduct, aligns with green chemistry and circular economy principles, reduces waste generation, and contributes to developing affordable, effective adsorbents for water purification.

2.0 MATERIALS AND METHODS

2.1 Chemicals and Reagents

Chemicals used: $NaH_2PO_42H_2O$ (sodium dihydrogen orthophosphate dihydrate, 98%, Fisher Scientific International); $Na_2HPO_4 \cdot 2H_2O$ (disodium hydrogen phosphate dihydrate, 99.5%, Riedel-deHaën); H_3PO_4 (orthophosphoric acid, 85%, Loba Chemie, Mumbai, India); CH_3CH_2OH (ethanol, Scharlau, Spain); $NaHCO_3$ (sodium hydrogen carbonate, 99.7%, Loba Chemie, Mumbai, India); NaOH (sodium hydroxide, 97%, Loba Chemie, Mumbai, India); NaCl (sodium chloride, 99.5%, Loba Chemie, Mumbai, India); HCl (hydrochloric acid, 37%, Loba Chemie, Mumbai, India); Ceftriaxone (Theon Pharmaceuticals Ltd., H.P., India); I_2 (iodine resublimed, 99.5%, LAB TECH CHEMICALS, India); Starch (soluble, LAB TECH CHEMICALS, India); $Na_2S_2O_3 \cdot 5H_2O$ (sodium thiosulfate pentahydrate, 99%, LAB CHEM, India); KI (potassium iodide, 99%, Molaton Scientific, India).

2.2 Sample collection and preparation

Aframomum angustifolium fruits collected from Kasulu district were washed, peeled, and sun-dried for 7 days. The dried samples were then transported to Sokoine University of Agriculture laboratory, where they were ground into a fine powder using a blender, sieved through a 125 µm mesh, and stored in polyethylene bags.

2.3 Preparation of Activated Carbon (AC)

Activated carbon was prepared by soaking 30 g of powdered shells (FPAA) in 500 mL of 4 M phosphoric acid for 24 h. The mixture was filtered through 0.7 µm Whatman filter paper, placed in a crucible, and dried in an oven at 110 °C for 36 h. The dried material was carbonized at 600 °C for 1 h to obtain activated carbon (AC), then cooled for 1 h. The resulting AC was ground with a mortar and pestle, soaked in 20% ethanol-water for 5 h with stirring (100 rpm, room temperature), and filtered. To neutralize residual acid from phosphoric acid activation (AC-FPAA-H_3PO_4), the carbon was soaked in 500 mL of 1% sodium hydrogen carbonate ($NaHCO_3$) solution for 1 h. The AC-FPAA-H_3PO_4 was then washed with distilled water until pH 7 was constant. After oven-drying at 105 °C for 12 h and cooling, the AC-FPAA-H_3PO_4 was reground using a mortar and pestle, and stored in a centrifuge bottle within a polyethylene bag for characterization and adsorption experiments.

2.4 Adsorbent characterization

2.4.1 Percentage Yield

The percentage yield of AC-FPAA-H_3PO_4 was calculated using Equation 1 as the mass ratio of produced activated carbon to the washed, dried, and ground FPAA precursor material, multiplied by 100.

$$Percentage\ yield\ (\%) = \frac{w_1}{w_0} x\ 100 \quad (1)$$

Where w_0 is the mass of the washed, dried and ground sample of FPAA and w_1 is the mass of activated carbon produced.

2.4.2 Bulk Density

The bulk density of AC-FPAA-H_3PO_4 was determined by weighing an empty 10 mL measuring cylinder, filling it to the mark with activated carbon, and reweighing. The bulk density was calculated using **Equation 2**.

$$Bulky\ density = \frac{W_{AC}}{V_{AC}} \quad (2)$$

Where W_{AC} is the mass of the activated carbon and V_{AC} is the cylinder volume packed with activated carbon.

2.4.3 Moisture Content

Moisture content (hygroscopic property) was determined by weighing 1 g of AC-FPAA-H_3PO_4 (w_2) in a crucible (w_0) using a digital balance, drying at 105°C for 1 h, and reweighing the crucible with sample (w_1). Moisture content was calculated using Equation 3.

$$\text{Moisture content} = \frac{w_0 - w_1}{W_2} \times 100\% \quad (3)$$

Where w_0 is the mass of crucible containing original activated carbon before drying, w_1 is the mass of crucible containing activated carbon after drying and w_2 is the mass of original activated carbon.

2.4.4 Ash Content

Ash content was determined by weighing 1 g of AC-FPAA-H_3PO_4 (w_3) in a crucible (w_1), heating in a furnace at 600°C for 2 h, and reweighing the crucible with residue (w_2). Ash content was calculated using Equation 4.

$$Ash\ content = \left(\frac{w_1 - w_2}{W_3}\right) \times 100\% \quad (4)$$

Where w_1 is the weight of crucible with activated carbon before heating, w_2 is the weight of crucible with activated carbon after heating and w_3 is the mass of original activated carbon added in the crucible.

2.4.5 Iodine Number

Iodine number was determined by titration where by 0.1 g AC-FPAA-H_3PO_4 was added to 100 mL of 0.05 M iodine solution, shaken at 150 rpm (25°C, 30 min), and filtered. For the sample titration, 10.0 mL of the filtrate was mixed with 5.0 mL KI and 1.0 mL HCl, and then titrated with

standardized 0.1 M $Na_2S_2O_3$ until pale yellow. After adding 2.0 mL starch indicator, titration continued until colorless. A blank titration used 10.0 mL of the original iodine solution. The iodine number was calculated using Equation 5.

$$Iodine\ number = \frac{(B-S) \times M \times 10000}{W} \quad (5)$$

2.4.5 Determination of point of zero charge (pHpzc) of AC-FPAA-H_3PO_4

The point of zero charge was determined using the batch equilibrium method (pH drift method). Solutions ranging from pH 2 to pH 12 were prepared using 0.1 M NaCl as the background electrolyte, with pH adjustment using 0.1 M HCl and 0.1 M NaOH. Then, 30 mg of FPAA-activated carbon was added to 40 mL aliquots of each pH solution. The mixtures were shaken for 24 h at 100 rpm and 25°C.

2.4.6 BET surface area

The BET surface analysis was conducted using Quantachrome NovaWin©1994-2013, Quantachrome Instrument v11.03 to determine the specific surface area of the adsorbent. The activated carbon and its raw materials of 0.0749 g each were used for the analysis.

2.4.7 Scanning electron microscope (SEM) and Energy-Dispersive X-ray Spectroscopy (EDAX) analysis

The surface morphology and elemental composition of the precursor materials (FPAA), activated carbon (AC-FPAA-H_3PO_4) before and after adsorption were analyzed using Scanning electron microscope (JOEL, JSM-6610LV).The small amount of sample was sprinkled on clean aluminium stub with carbon tape using a clean spatula. The stub was then placed in a sputter coater with Pd/Au turget. The stub was further placed to the SEM/EDS stage, secured and pumped down to the vacuum.

2.4.8 Fourier-transform infrared spectroscopy (FTIR) analysis

The functional groups of the precursor materials (FPAA) and adsorbent **(**AC-FPAA-H_3PO4) was analyzed using IRAffinity-1S Fourier transform infrared spectrophotometer-SHIMADZU. A small amount of activated carbon was mixed with 100 mg of potassium bromide (KBr) in a mortar and pestle. The mixture was compressed in the machine to obtain a pellet sample that was placed in a cell for the analysis.

2.5 Adsorption experiments

Before adsorption experiment, 1000 mg/L of ceftriaxone solution was prepared using phosphate buffer solution and then serial dilution was made to obtain the required concentration**.** The known mass of activated carbon (AC-FPAA-H_3PO_4) was added in 5 mL of known concentration of ceftriaxone solution and shaken at 100 rpm for 1 h. Thereafter, the mixture of activated carbon and ceftriaxone solution was filtered using 0.7 µm Whatman filter paper to obtain solution that was used for measurement of ceftriaxone concentration. The concentration of ceftriaxone before and after adsorption was determined by scanning the solution using 6715 UV/Vis Spectrophotometer (JENWAY). The optimization of parameters including pH, temperature, ceftriaxone concentration and dosage of AC-FPAA-H_3PO_4 at agitation speed of 100 rpm and contact time of 1 h were studied. The removal efficiency and adsorption capacity at equilibrium were calculated using the equations 6 and 7 respectively.

$$RE\ \% = \frac{(Co - Ce)}{Co} x\ 100 \quad (6)$$

$$q_e = (C_O - C_e)\ X \frac{v}{m} \quad (7)$$

Where q_e is the adsorption capacity, *RE %* is the removal efficiency, *Co* is the initial concentration, C_e is the concentration of ceftriaxone at equilibrium, *v* is the volume of adsorbate solution and *m* is the mass of adsorbent.

2.6 Adsorption isotherms

The Langmuir, and Freundrich isotherm models were evaluated using adsorption data at ceftriaxone concentrations from 20 mg/L to 1000 mg/L, adsorbent dose-adsorbate solution of 0.1 g/5 mL, solution pH of 2, and contact period of 1 h as an optimal experimental conditions. The equations 8 and 9 were applicable for Langmuir equation while equation 10 was applicable for Freundlich model

$$\frac{1}{q_e} = \frac{1}{qmax} + \frac{1}{K_L q_{max}} x \frac{1}{C_e} \quad (8)$$

$$R_L = \frac{1}{1 + K_L q_{max} \times C_o} \quad (9)$$

$$\log q_e = \log K_F + \frac{1}{n}\ x \log C_e \quad (10)$$

Where C_o is the initial concentration of ceftriaxone, q_e is the ceftriaxone concentration at equilibrium, C_e is the concentration of ceftriaxone at equilibrium, q_{max} is the ceftriaxone monolayer's maximum adsorption, K_L is the Langmuir constant which is related to energy of adsorption, R_L is the ceftriaxone and activated carbon (AC-FPAA-H_3PO_4) affinity, and K_F is the Freundlich constant, n is the Freundrich index which shows the degree of adsorption and surface heterogeneity.

2.7 Kinetics studies

Kinetics study was evaluated using adsorption at different time (from 0 to 480 s) at 500 mg/L ceftriaxone concentration, 0.1 g /100 mL of adsorbent-adsorbent, 100 rpm and 298.15 K. The four kinetic models (pseudo-first order, pseudo-second order, Elovich and Weber's intraparticle diffusion) were evaluated using equations 11, 12, 13 and 14 respectively.

$$log(q_e - q_t) = \log q_e - \frac{k_1 t}{2.303} \quad (11)$$

$$\frac{t}{q_t} = \frac{1}{k_2 q_e^2} + \frac{t}{q_e} \quad (12)$$

$$q_{t=} \frac{1}{\beta}\ln(\alpha\beta) + \frac{1}{\beta}\ln(t) \quad (13)$$

$$q_t = k_i t^{0.5} + C_i \quad (14)$$

where q_e (mg/g) is the amount adsorbate adsorbed at equilibrium, q_t (mg/g) is the amount of adsorbate adsorbed at any time, t (s) is the adsorption time, k_1 is the first rate constant, k_2 is the second rate constant, α is the initial adsorption rate (mg/g min), β is desorption constant, which is related to the surface coverage and activation energy of chemisorption (mg/g), k_i is the intraparticle diffusion rate constant and C_i is the thickness of boundary layer.

2.8 Thermodynamic study

Thermodynamic parameters (i.e. enthalpy, Gibbs free energy and entropy) was evaluated by carrying adsorption experiment at 20 mg/L ceftriaxone solution, 0.1 g of activated carbon, 100 rpm, pH 2 and for 1 h at different temperature (298.15 K, 308.15 K, 318.15 K, 328.15 K and 338.15

K). The determination of enthalpy, Gibbs free energy and entropy changes involved the equation 15, 16 and 17 below.

$$K = \frac{C_a}{C_e} \quad (15)$$

$$\Delta G = -RT ln\, K \quad (16)$$

$$\ln K = \frac{\Delta S}{R} - \frac{\Delta H}{RT} \quad (17)$$

Where K is the equilibrium constant, C_e is adsorbate concentration remaining in the solution (mg/L), C_a is the adsorbate concentration adsorbed at equilibrium (mg/L), R is the universal gas constant, T is the temperature (K), ΔG is the change in Gibbs free energy, and ΔH is enthalpy change and ΔS is the entropy change.

3.0 RESULTS AND DISCUSSION

3.1 Characterization

3.1.1 Percentage yied, bulky density, moisture content, ash content and iodine number of Activated carbon

The characterization results of the activated carbon (AC-FPAA-H_3PO_4), as presented in **Table 1**, revealed a percentage yield of 25.97%, bulk density of 0.186 g/mL, moisture content of 15%, ash content of 2.88%, and iodine number of 700 mg/g. The relatively low values of bulk density, ash content, and moisture content suggest that the material possesses desirable characteristics for broad adsorption applications. The activated carbon with ash content ranging from 1% to 20% is suitable for the adsorption of various contaminants [20]. Therefore, the ash content of 2.88% confirms that the synthesized activated carbon meets the quality standards for effective adsorption, including that of antibiotics. Moreover, the iodine number of 700 mg/g falls within the accepted range for high-quality activated carbon (500–1200 mg/g), as reported by Ceyhan et al. (2013) and María Lorena et al. (2025) [21, 22]. This further indicates a favourable microporous structure, supporting its effectiveness in adsorbing small molecules such as ceftriaxone. These preliminary findings confirm that the AC-FPAA-H_3PO_4 material prepared in this study was well-suited for adsorption applications, and thus, it was used for subsequent experiments involving the removal of ceftriaxone from an aqueous solution.

Table 1, yield, bulky density, moisture content, ash content and iodine number of AC-FPAA-H_3PO_4

Parameter	Value	Standards	Reference
Carbon yield (%)	25.97	Min 30%	[23]
Bulky density (g/mL)	0.186	0.30-0.35 gcm^{-3}	[23]
Moisture content (%)	15	max.15	[24]
Ash content (%)	2.88	max. 10	[24]
Iodine number (mg/g)	700	500-1200	[21]

3.1.2 Point of zero charge (pHpzc) of activated carbon (AC-FPAA-H_3PO_4)

The surface charge of an adsorbent plays a significant role in determining the nature of its interaction with a target analyte. The point of zero charge (pHpzc) corresponds to the pH at which the number of positive and negative charges on the adsorbent surface are equal [25]. Thus, the pHpzc of the synthesized activated carbon (AC-FPAA-H_3PO_4) was determined, and the results (**Fig. 1**) revealed a pHpzc value of 4.5. This indicates that the surface of AC-FPAA-H_3PO_4 is electrically neutral at pH 4.5. At pH values below 4.5, the surface carries a net positive charge, while at pH values above 4.5, the surface becomes negatively charged. This behavior influences the electrostatic interactions between the adsorbent and charged species in solution. Similar pHpzc values have been reported in previous studies for activated carbon derived from various biowastes, including mango leaves (pHpzc = 4.6), coconut leaves (pHpzc = 3.2), and watermelon rind (pHpzc = 4.1) [26, 27]. These comparisons support the characterization of AC-FPAA-H_3PO_4 as a viable adsorbent with predictable charge behavior across different pH levels.

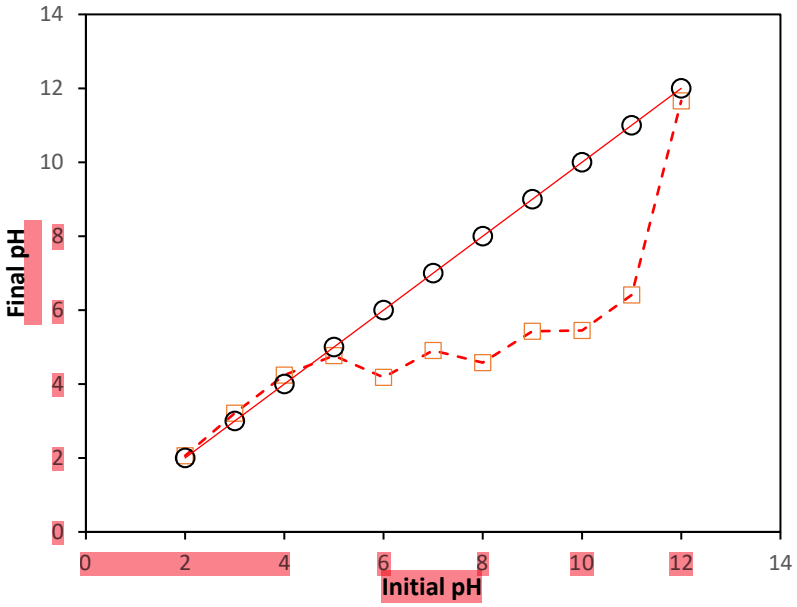

Fig.1: The point of zero charge (pHpzc) plot of AC-FPAA-H_3PO_4

3.1.3 BET Analysis

The Brunauer-Emmett-Teller (BET) surface area provides a quantitative measure of the total surface area available for adsorption on a material. As shown in **Table 2**, the BET analysis revealed that the prepared activated carbon (AC-FPAA-H_3PO_4) exhibited a significantly higher surface area of 1895.646 m^2/g compared to its raw precursor material, FPAA, which had a surface area of 335.809 m^2/g. This considerable increase suggests that AC-FPAA-H_3PO_4 possesses a much greater number of adsorption sites, thereby enhancing its adsorption potential for pollutant molecules [28-31]. The activated carbon with surface area of greater than 1000 m^2/g is considered efficient for the removal of different organic pollutants from aqueous solutions [32]. Additionally, the activation process resulted in an increase in total pore volume, average pore size, pore volume, pore diameter and pore surface area (**Table 2**). The average pore radius increased from 0.522 nm in FPAA to 0.657 nm in AC-FPAA-H_3PO_4, indicating that the activated carbon provides sufficient spatial accommodation for adsorbate molecules. Moreover, the pore volume nearly doubled, increasing from 1.186 cm^3/g to 2.292 cm^3/g, which further supports the enhanced adsorption capacity. Pore volume reflects the total vacant space available within the adsorbent. The pore volume increased from 0.292 cm^3/g of precursor materials (FPAA) to 1.653 cm^3/g of the adsorbent. As well, pore surface area increased from 185.874 cm^3/g of precusor materials (FPAA) to 741.849 cm^3/g for the activated carbon (AC-FPAA-H_3PO_4).

Therefore, the increased pore volume and its suface area means that there is enough space and sites with great ability to capture and retain adsorbate molecules. The presence of a larger pore network facilitates faster diffusion of antibiotic molecules into the adsorbent, improving the overall efficiency of the adsorption process. The pore diameter increased from 1.6954 nm of precursor materials (FPAA) to 1.7030 nm of the adsorbent, means that the adsorbent has more micropores with few mesopores. Finally, the nature of adsorption isotherm shape suggests the AC-FPAA-H_3PO_4 involve type II isotherm as shown in **Fig.S3** [33, 34]. This means that both monolayer and multilyer adsorption probably occur on the adsorbent as well as physisorption type of adsorption mechanism. The adsorption involving both monolayer and multilayer can be supported by presence of both micropores and mesopores as well as other surface chemistry of the adsorbents.

Table 2: BET surface area, avarage pore size and total pore volume.

Material	Surface area (m^2/g)	Average pore size (nm)	Total pore volume (cm^3/g)	Pore volume (cm^3/g)	Pore diameter (nm)	Pore surface area (m^2/g)
FPAA	335.809	0.522	1.186	0.292	1.6954	185.874
AC-FPAA-H_3PO_4	1895.646	0.657	2.292	1.653	1.7030	741.849

3.1.3 SEM-EDAX analysis

As shown in **Fig.2a** FPAA showed irregular huge blocks and aggregations with smooth surfaces. However, the activated carbon **(Fig.2b)** changed into rough aggregates with pores of different diameters. This probably was developed due to chemical activation and physical activation of the FPAA as a precursor materials [35-37]. The destructed and clogged pores surfaces were observed for the adsorbent after adsorption **(Fig.2c)**. This was a possible indicator that ceftriaxone molecules were adsorbed into the pores of the adsorbent [38]. The findings also indicate that the pores were not completely filled with the adsorbed molecules. This is a possible indicator for the reusability of the fabricated activated carbon without the need for the regeneration of the active sites.

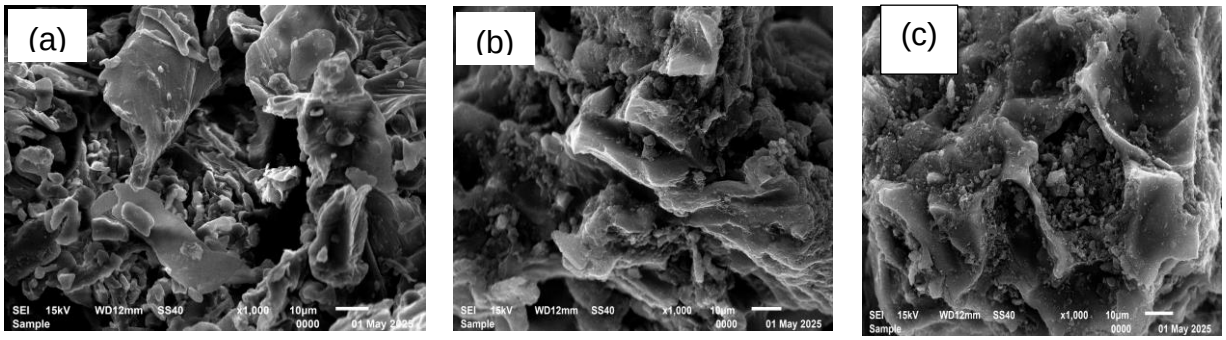

Fig.2: SEM images.(a) FPAA (b) AC-FPAA-H_3PO_4 (c) AC-FPAA-H_3PO_4 after adsorption

Elemental compositions of the precursor material (FPAA), the adsorbent before adsorption (AC-FPAA-H_3PO_4), and the adsorbent after adsorption are shown in **Fig. S2** and **Table 3**. The findings showed that FPAA precursor composition composed of C (49.96%), N (2.07%), O (46.72%), Mg (0.49%), P (0.18%), K (0.4%), Mn (0.06%), and Fe (0.05%) while the AC-FPAA-H_3PO_4 adsorbent composed of C (79.40%), N (11.12%), O (6.66%), P (2.43%), K (0.19%), Mn (0.09%), and Fe (0.09%). The increase in carbon content for the activated carbon (49.96% to 79.40%) demonstrates that chemical activation with phosphoric acid and physical activation at 600°C enhanced carbon formation. The decrease in oxygen (46.72% to 6.66%) further indicates effective removal of volatile compounds during the activation to produce a porous surface. The increase in nitrogen (2.07% to 11.12%) and phosphorus (0.18% to 2.43%) were also observed for the post-adsorption activated carbon, consistent with previous reports [39, 40]. Post-adsorption, the adsorbent also showed new element such as sulfur (0.20%) and sodium (0.32%). Increases in nitrogen (11.12% to 11.80%) and oxygen (6.66% to 9.39%) are possibly attributed to adsorbed ceftriaxone.

Table 3: Elemental composition of precursor and activated carbon before and after adsorption.

Element	FPAA	Pre adsorption AC-FPAA-H_3PO_4	Post adsorption -FPAA-H_3PO_4
C	49.96	79.40	75.54
N	2.07	11.12	11.80
O	46.72	6.66	9.39
S	-	-	0.20
Cl	-	-	0.10

***elemental compositions are in weight percentage (wt%)**

3.1.4 FTIR analysis

The FTIR analysis was used to study the surface chemistry of precursor materials and activated carbon. The results (**Fig. 3&Table S1)** showed a broad peak at 3346 cm^{-1}, associated with O-H stretching vibrations in alcohols or phenols [41, 42], and a sharp peak at 3651 cm^{-1}, attributed to free O-H groups [43]. Peaks observed at 1029 cm^{-1} were associated with C-N stretching vibration [39, 44], while the peak at 1249 cm^{-1} likely indicates C-O stretching vibration from ethers or carboxylic groups [39]. Additionally, peaks at 1380 cm^{-1}, 1612 cm^{-1}, and 1722 cm^{-1} correspond to stretching vibrations of CH_3, C=C, and C=O groups, respectively [39]. Conversely, the broad O-H peak (3346 cm^{-1}) was absent in the phosphoric acid-activated carbon (AC-FPAA-H_3PO_4) (**Fig. 3b**), indicating functional group modification during the activation process. The adsorbent material also exhibited a peak at 954 cm^{-1}, related to =C-H bending [45], which was not prominent in the precursor material (FPAA), further demonstrating functional group modification. Peaks at 1466 cm^{-1} and 1570 cm^{-1} were associated with the C=C bonds of aromatic rings [46]. However, similar peaks were observed in the activated carbon at 1072 cm^{-1} (P-O-P) [39], 1381 cm^{-1} (C-H) [44,45], 2980 cm^{-1} (C-H), and 3657 cm^{-1} (free O-H) [43]. The distinct peaks at 1461 cm^{-1} and 1570 cm^{-1} likely indicate hydrocarbons. The presence of multiple weak peaks between 405–825 cm^{-1} also signifies C-C bonds [43].

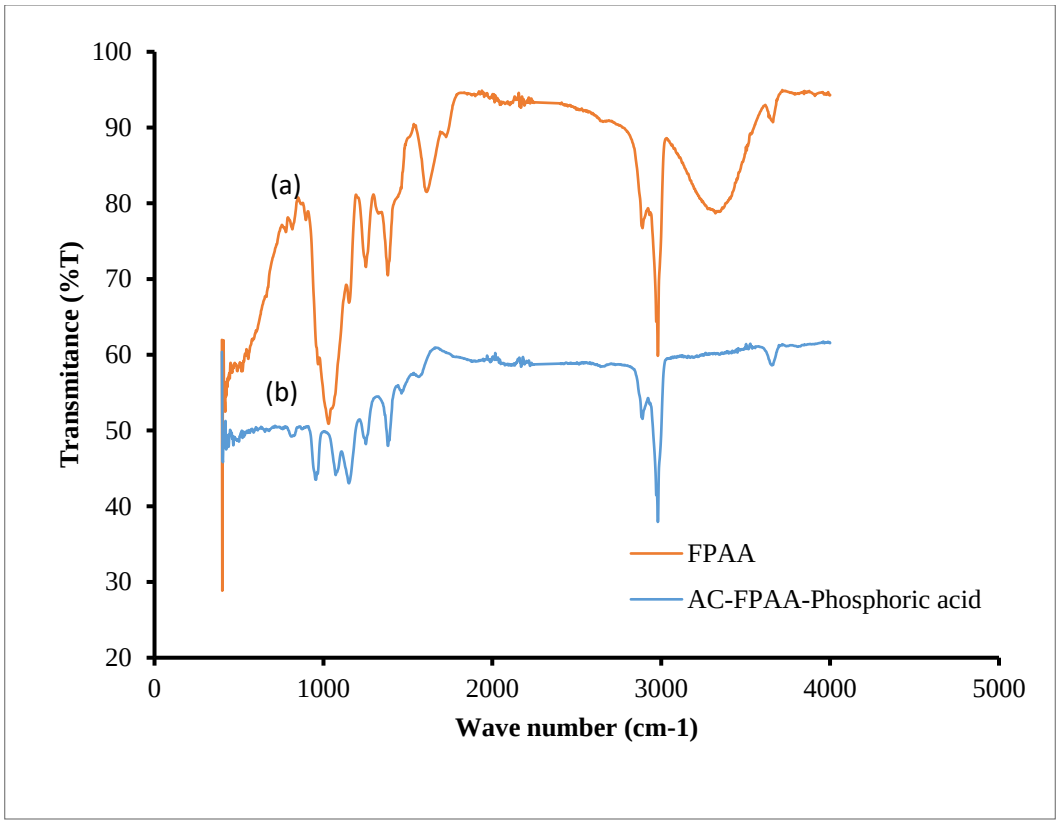

Fig.3. FTIR results (a) FPAA (b) AC-FPAA-H_3PO_4

3.2 Adsorption studies

3.2.1 Effect of pH on adsorption of ceftriaxone

pH plays a crucial role in the adsorption process, as it influences the speciation of the adsorbate in solution [47]. Thus, the effect of pH on the adsorption of ceftriaxone was investigated in the current study. As illustrated in **Fig. 4**, the adsorption efficiency (RE%) of ceftriaxone increased from 82% to 95% as the pH increased from 1 to 2. Beyond pH 2, further increases in pH led to a gradual decline in the adsorption efficiency, reaching a minimum of 80% at pH 8. The lower adsorption efficiency observed at pH 1 may be attributed to electrostatic repulsion between the positively charged ceftriaxone molecules **Fig. S1 a**) and the positively charged surface of the activated carbon. Similarly, the reduced adsorption efficiency at higher pH levels could be due to increased electrostatic repulsion between negatively charged ceftriaxone species (**Fig. S1 c**) and the negatively charged activated carbon surface The maximum adsorption efficiency of 95% was recorded at pH 2, where ceftriaxone predominantly exists in its zwitterionic form (**Fig. S1 b**), while the activated carbon surface retains a positive charge. This observation suggests that the adsorption of ceftriaxone onto the activated carbon surface was primarily governed by

electrostatic attractions between the cetriaxone and activated carbon. However, the role played by weak intermolecular interactions such as Van der Waals forces, dipole–dipole interactions, and dispersion forces can not completely rules out. Comparable results were reported by Badi et al. (2018) [37], where a removal efficiency of 97.18% was achieved using Fe_3O_4-modified activated carbon at a slightly acidic pH of 3.14. Therefore, based on the results in **Fig. 4**, the optimal removal efficiency of 95% was obtained using a buffer solution at pH 2.

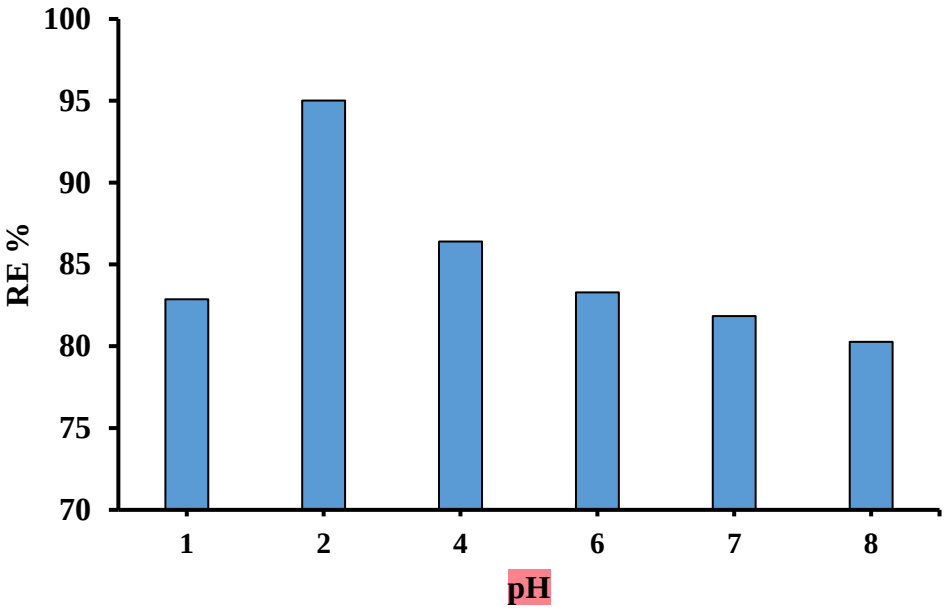

Fig.4: Effect of pH on adsorption of ceftriaxone. Experiemntal conditions: pH 2, mass of adsorbent (0.1 g), concentration of ceftriaxone (20 mg/L), agitation speed (100 rpm), temperature (298.15 K) and contact time (1 h).

3.2.3 Effect of concentration of ceftriaxone

The effect of the initial concentration of ceftriaxone on adsorption efficiency was investigated, and the results are presented in **Fig.6**. An initial increase in ceftriaxone concentration from 20 mg/L to 200 mg/L resulted in an increase in removal efficiency from 95% to 97.8%. However, as the concentration further increased from 200 mg/L to 1000 mg/L, the adsorption efficiency declined slightly to 94.5%. The initial rise in efficiency can be attributed to an increased concentration gradient, which enhances the driving force for mass transfer between the liquid phase and the solid adsorbent, thereby promoting adsorption [48]. Nevertheless, the mass of activated carbon

used (100 mg) remained constant throughout the experiment, resulting in a fixed number of available adsorption sites. At higher initial concentrations, these sites likely became saturated, limiting further adsorption and causing a decline in removal efficiency. This saturation of adsorption sites, coupled with possible pore blockage, may have contributed to the reduced efficiency observed at higher concentrations [42]. Therefore, based on these findings, an initial concentration of 200 mg/L was determined to be the optimal condition for effective ceftriaxone adsorption in this study.

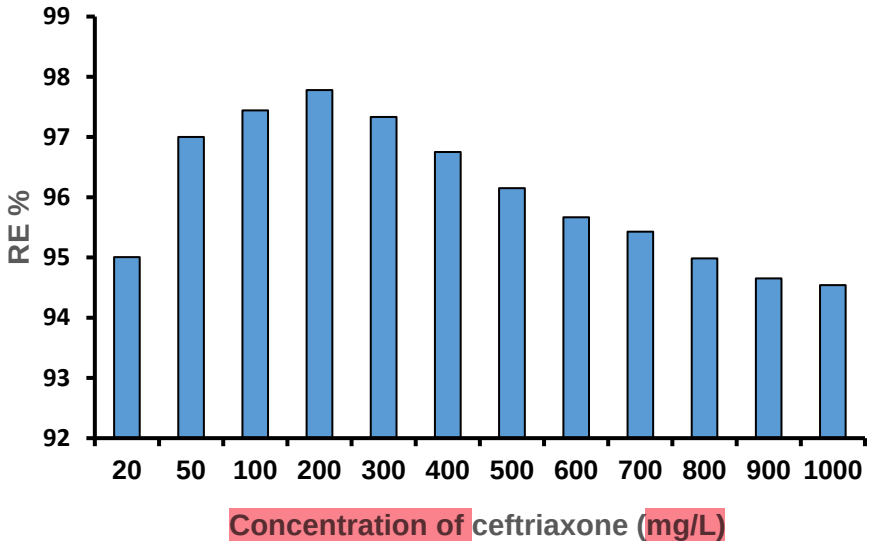

47

Fig.6: Effect of concentration on adsorption of ceftriaxone. Experimental conditions: pH 2, temperature (298.15 K), stirring speed (100 rpm), 5 mL of initial centriaxone (20-1000 mg/L) and mass of adsorbent (0.1 g).

12

3.2.4 Effect of dosage on adsorption of ceftriaxone

60

The effect of adsorbent dosage on the removal efficiency of ceftriaxone using AC-FPAA-H_3PO_4 was evaluated, as presented in **Fig. 7**. The results showed that increasing the dosage from 2 g/L to 20 g/L led to only a marginal increase in removal efficiency, from 94.67% to 95.05%. This insignificant change suggests that AC-FPAA-H_3PO_4 possesses a high adsorption capacity,

enabling it to achieve high removal efficiency even at low dosages. This behavior is likely due to the abundance of available adsorption sites within the material, which allows effective removal of the antibiotic even with a minimal amount of adsorbent. These findings contrast with other reported studies, where adsorption efficiency typically increases with dosage up to an optimum point, after which it either plateaus or decreases. For instance, Rahmawati et al. (2024) reported that the removal efficiencies of ceftriaxone and ciprofloxacin using graphene oxide derived from corn cob increased with adsorbent mass up to optimal levels of 40 mg and 20 mg, respectively [42]. Similarly, Alawa et al. (2025) observed increased removal of ciprofloxacin from water with increasing dosages of biochar derived from agricultural waste biomass, which had BET surface areas of 274 m^2/g (CWS) and 219 m^2/g (AWS) [44].The unusual high BET surface area of AC-FPAA-H_3PO_4 (1895.646 m^2/g) may explain this deviation from the typical trend. The extensive surface area is likely to provide sufficient active sites to accommodate large quantities of adsorbate, even at low dosages. Therefore, AC-FPAA-H_3PO_4 possess unique structural features that enable it to maintain high adsorption efficiency regardless of dosage, making it a highly efficient and economical adsorbent.

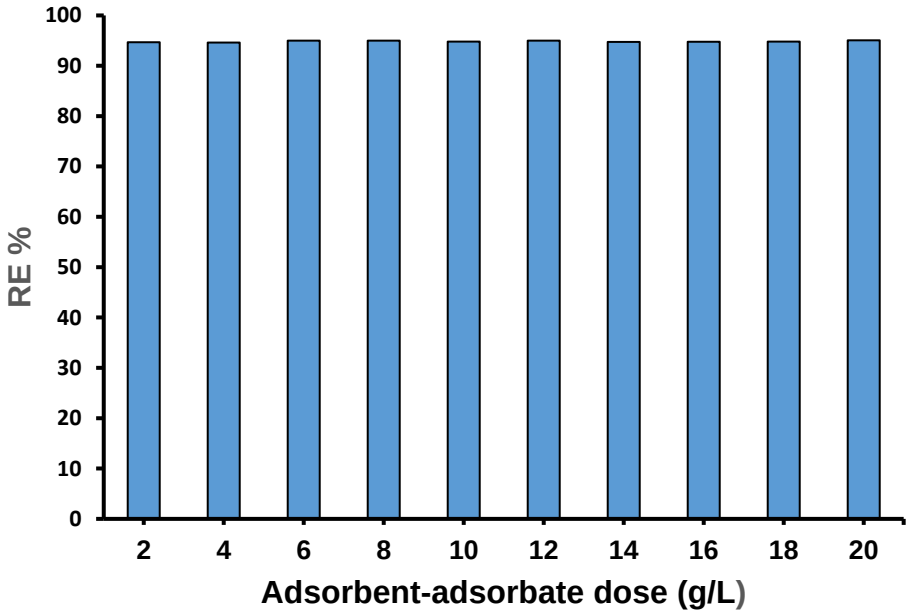

Fig.7: Effect of adsorbent dosage. Experimantal conditions: pH 2, concentration of ceftriaxone (20 mg/L), stirring speed (100 rpm), temperature (298.15 K) and contact time (1 h).

3.2.2 Effect of temperature on adsorption of ceftriaxone

Temperature is a critical parameter influencing adsorption processes, as temperature variations can affect the chemical interactions between the adsorbent and adsorbate. In this study, the removal efficiency of ceftriaxone decreased slightly from 95% to 92% as the temperature increased from 298.15 K to 338.15 K (**Fig. 5**). This decline suggests that the adsorption of ceftriaxone onto AC-FPAA-H_3PO_4 is exothermic in nature, indicating that lower temperatures favour the adsorption process [49]. The reduction in adsorption efficiency at elevated temperatures may be attributed to enhanced desorption and weaker interactions between ceftriaxone and the activated carbon surface. At higher temperatures, the affinity between ceftriaxone and the surrounding solution increases, while its interaction with the adsorbent decreases [50]. These findings are consistent with other reported studies on the adsorption of organic pollutants. For instance, Naghipour et al. (2024) observed a similar temperature-dependent decrease in ceftriaxone removal using Fe_2O_3-magnetized kaolin [51]. Comparable behavior has also been reported in the removal of amoxicillin using Aloe barbadensis Miller-based bioadsorbents [52], ciprofloxacin removal using biochar derived from agricultural waste [44]. These studies collectively support the conclusion that lower temperatures enhance adsorption efficiency for various organic pollutants.

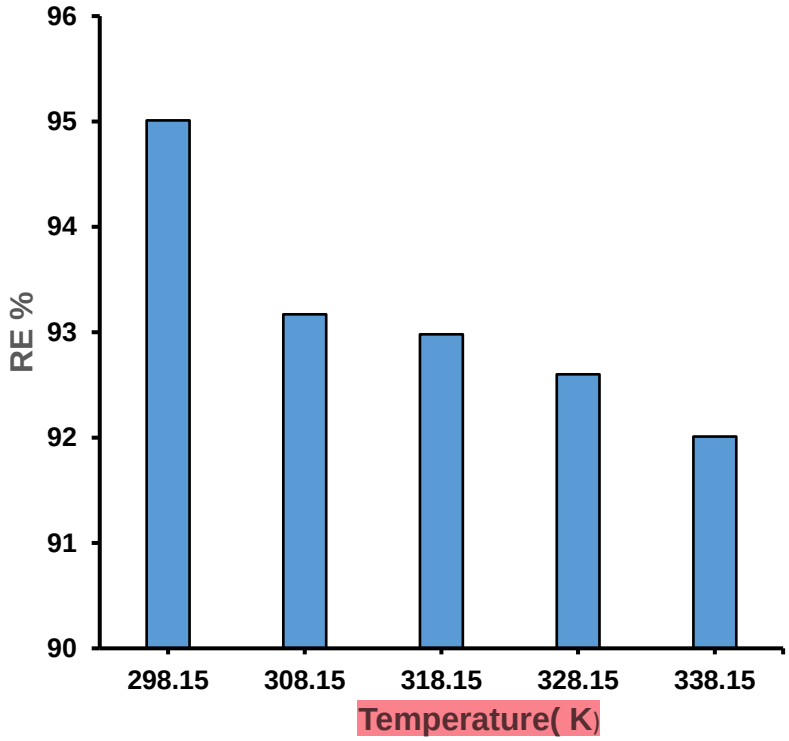

Fig.5: Effect of solution temperature on adsorption of ceftriaxone. Experimental condition: pH 2, mass of adsorbent-adsorbate solution (0.1 g/5 mL), concentration of ceftriaxone (20 mg/L), stirring speed (100 rpm), contact time (1 h) and tempreture 298.15 – 338.15 K.

3.3 Adsorption isotherms for adsorption of ceftriaxone

The results in **Fig 9 and Table S2** shows R^2 values for both Langmuir and Freundlich of 0.9862 and 0.9833 respectively. The observation is a possible indicator that the adsorption of the antibiotic followed the two models. The other parameters related to Langmuir isotherm model obtained are q_{max} of 72.99 mg/L, K_L of 0.02937 L/g and R_L of 0.145. The other parameters released to Freundlich isotherm are K_F value of 3.119 L/mg and n value of 1.5225. The value of K_L being small, that is 0.02937 L/g probably indicates the existence of weak forces between adsorbent and adsorbate molecules. As well, high value of n (1.5225) means there is stronger interaction between ceftriaxone molecules and activated carbon. Similar findings were previously reported on the removal of industrial dye using activate carbon from Himalayan char pine biomass [53].

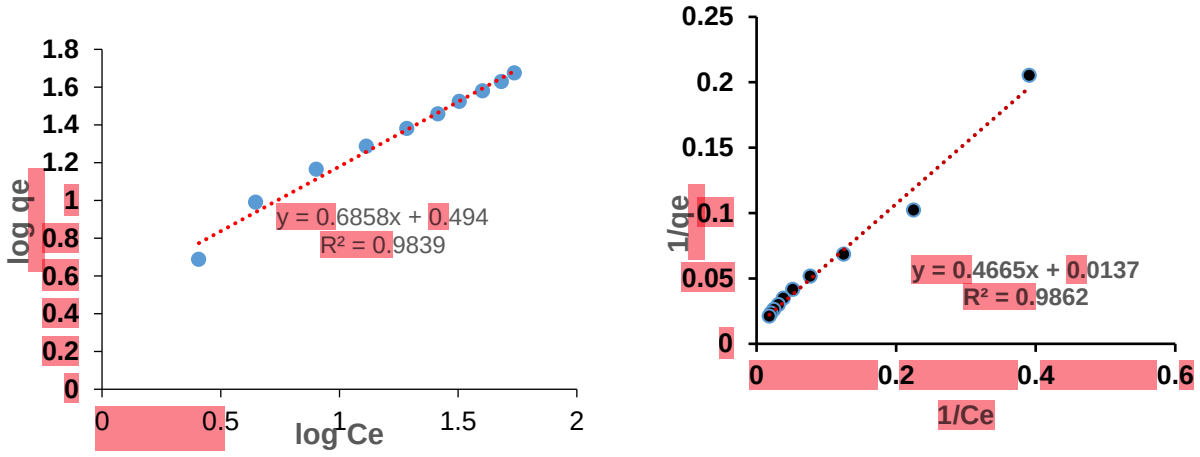

Fig.9: Isothermal models; (a) Freundlich isothermal model (b) Langmuir isotherm model. Experimental conditions: Experimental conditions: pH 2, temperature (298.15 K), stirring speed (100 rpm), 5 mL of initial centriaxone (20-1000 mg/L) and mass of adsorbent (0.1 g).

3.4 Adsorption kinetics of ceftriaxone antibiotic

The results presented in **Fig.10** and **Table S3** show that the regression coefficient (R^2) values for the kinetic models were 0.90 for the pseudo-first-order, 0.98 for the pseudo-second-order, 0.90

for the Elovich model, and 0.97 for the Weber's intraparticle diffusion model. The predicted equilibrium adsorption capacity (q_e) for the pseudo-second-order model was 434.76 mg/g, closely aligning with the experimentally determined qe value of 435.87 mg/g. The observation indicates that the adsorption is likely to be governed by chemisorption mechanisms by involving valence forces through either sharing or exchange of electrons between ceftriaxone molecules and activated carbon. In contrast, the pseudo-first-order model yielded a predicted q_e of 265.46 mg/g, significantly lower than the experimental value (435.87 mg/g). For the Weber's model, the boundary layer thickness constant (C_i) was calculated as 195.89. The high R^2 values for the pseudo-second-order (0.98) and Weber's intraparticle diffusion model (0.97) probably means that the adsorption of ceftriaxone onto AC-FPAA-H_3PO_4 likely follows both pseudo-second-order kinetics and intraparticle diffusion mechanisms. Moreover, the close agreement between the predicted and experimental q_e values in the pseudo-second-order model further supports this conclusion. The large C_i value (195.89) indicates a significant boundary layer effect, suggesting that external mass transfer resistance may influence the diffusion of ceftriaxone molecules into the pores of the activated carbon. These findings are consistent with previous studies where the adsorption of ceftriaxone onto activated carbon modified with magnetic Fe_3O_4 nanoparticles followed pseudo-second-order kinetics [37].

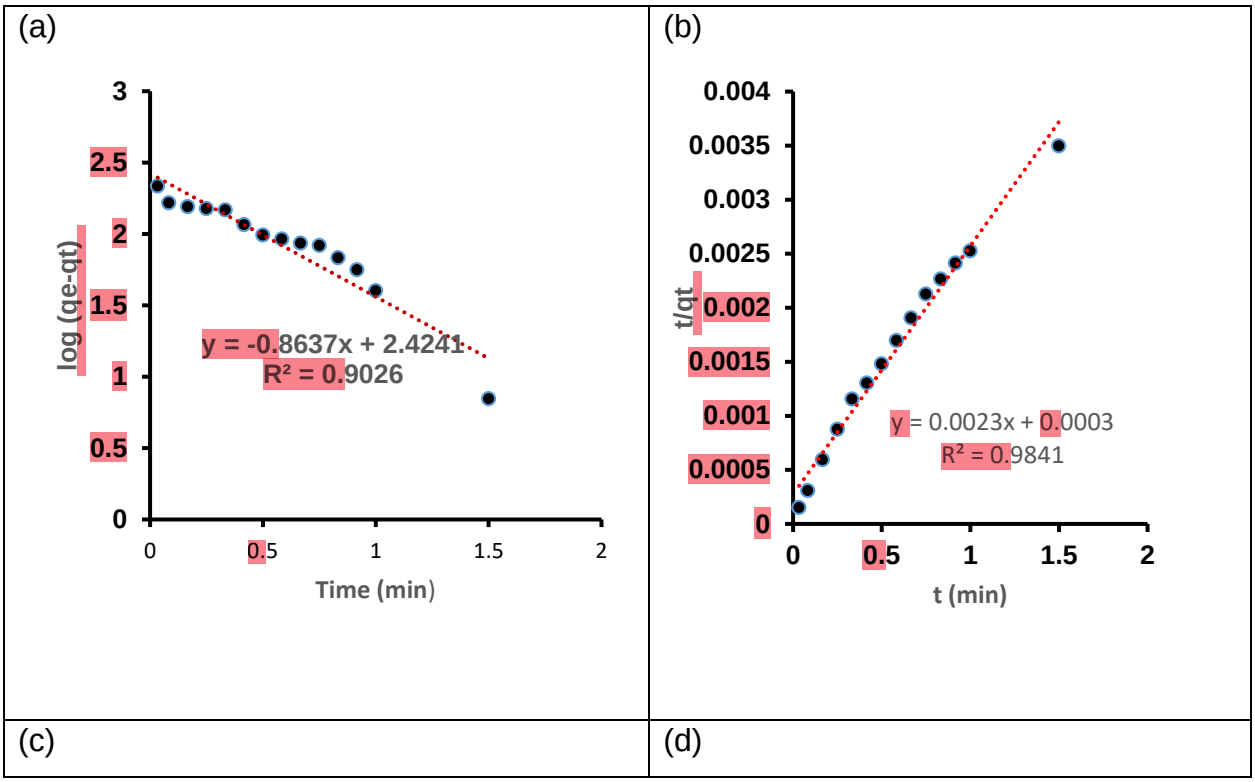

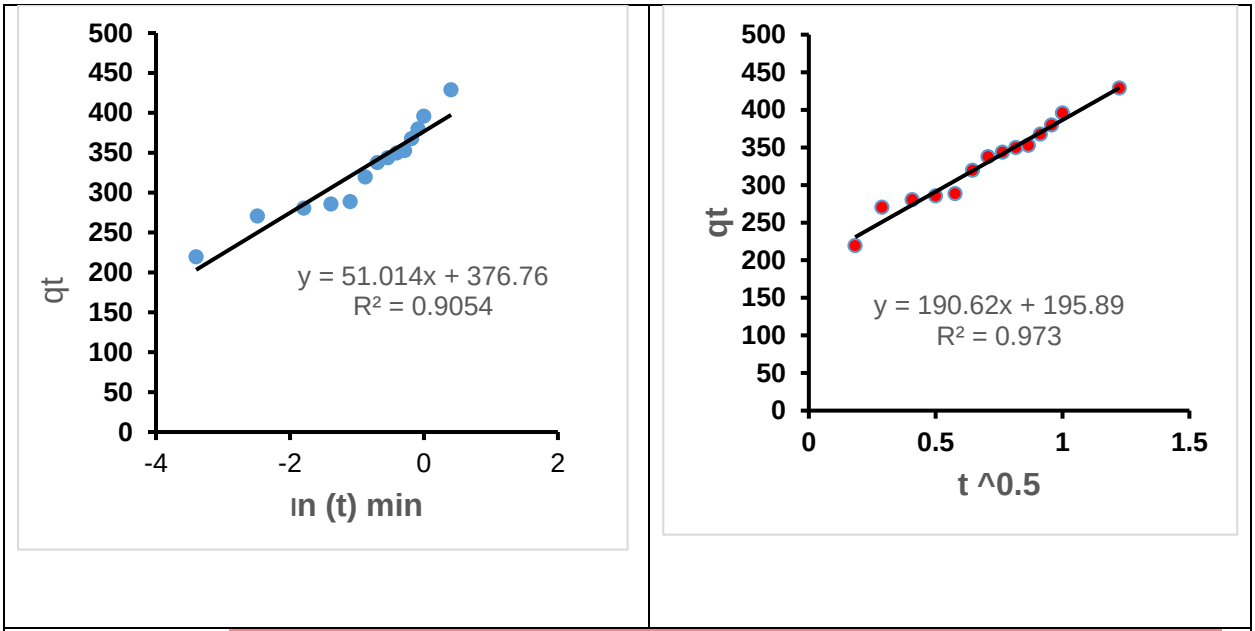

Fig.10: Kinetics models: (a) Pseudo-first order (b) Pseudo-second order (c) Elovich (d) Weber's model. Experimental conditions: pH 2, adsorbent mass (0.1 g), initial concentration of ceftriaxone solution (500 mg/L), stirring speed (100 rpm) and temperature (298.15 K).

3.5 Thermodynamic study

The thermodynamic parameters presented in **Table 4** & **Fig. 3S** indicate that the enthalpy change (ΔH) and entropy change (ΔS) for the adsorption of ceftriaxone using AC-FPAA-H_3PO_4 were −4.4292 kJ·mol^{-1} and 7.691 J·mol^{-1}·K^{-1}, respectively. The Gibbs free energy changes (ΔG) at various temperatures 298.15 K, 308.15 K, 318.15 K, 328.15 K, and 338.15 K were found to be −6.8270, −6.6946, −6.8359, −6.8917, and −7.1390 kJ·mol^{-1}, respectively. The average ΔG value of −6.7980 kJ·mol^{-1} across these temperatures suggests that the adsorption process occurs spontaneously under the studied conditions.

The negative value of ΔH confirms that the adsorption process is exothermic, while the positive value of ΔS indicates an increase in randomness at the solid-solution interface during the adsorption. Additionally, the positive ΔS also suggests a high affinity of the activated carbon toward ceftriaxone molecules, as greater disorder typically reflects favorable adsorbate-adsorbent interactions. These findings are consistent with previous studies on the thermodynamics of adsorption processes [54]. Overall, the thermodynamic data demonstrate that ceftriaxone removal using AC-FPAA-H_3PO_4 is both feasible and favorable at room temperature, highlighting its potential for industrial-scale application without the need for extensive temperature regulation.

Table 4. Summary of thermodynamic parameters.

Temperature (K)	ΔG (kJ.mol $^{-1}$)	ΔH (kJ.mol^{-1})	ΔS (J.mol^{-1} K^{-1})
298.15	-6.82709	-4.4292	7.69128
308.15	-6.69460		
318.15	-6.83593		
328.15	-6.89166		
338.15	-7.13898		

3.6 Application of AC-FPAA-H_3PO_4 for real water samples

Real water samples were collected from the Ngerengere River near Solomon Mhalangu Campus in Mazimbu and from a well at the Free Pentecostal Church of Tanzania (FPCT)-Kihonda Magorofani, within Morogoro Municipality's Kihonda Ward. Before the adsorption experiments, the water samples' conductivity and pH were measured and recorded (**Table S4**). The results (**Fig. 11**) showed removal efficiencies of 97.47% for distilled water, 98.61% for river water, and 97.15% for well water in the first cycle, indicating that coexisting constituents in real water samples had minimal impact on AC-FPAA-H_3PO_4's adsorption efficiency. The reusability was evaluated to assess practical applicability and reduce costs/environmental impact. After each cycle, spent adsorbent was centrifuged, decanted, and dried at 90°C for one hour. **Fig. 11** shows declining removal efficiency with increasing cycles: from 97.92% (Cycle 1) to 65.04% (Cycle 5) for distilled water, 99.36% to 88.05% for river water, and 96.92% to 90.44% for well water. This reduction likely resulted from progressive pore blockage by accumulated ceftriaxone molecules, suggesting multilayer formation consistent with earlier observations in the current study Although AC-FPAA-H_3PO_4 remained effective through five reuse cycles, adding desorption step could improve long-term performance, though adsorbent loss during regeneration may affect efficiency.

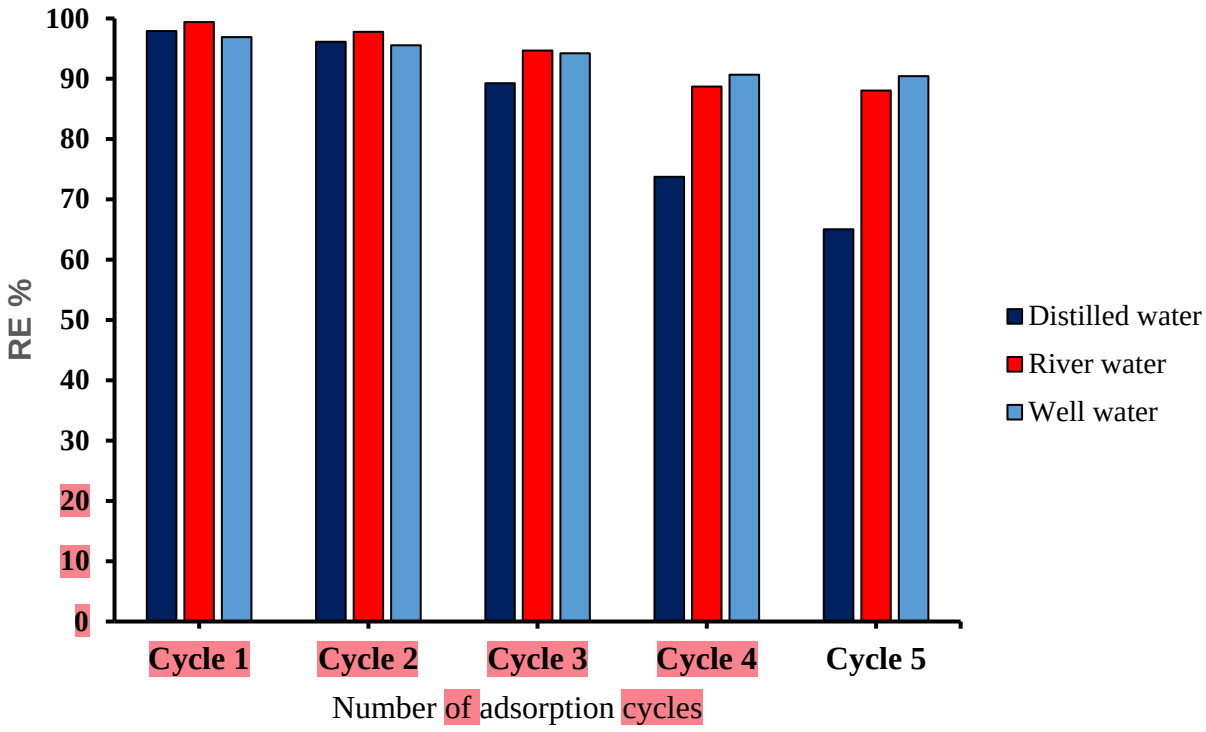

Fig.12: Removal efficiencies for reused adsorbent in five cycles. Experimental conditions: Adsorbent mass (0.1 g), 10 mL of ceftriaxone concentration (200 mg/L), stirring speed (100 rpm), temperature (298.15 K), and contact time (1 hour).

3.7 Comparability of AC-FPAA with other adsorbents

The performance of AC-FPAA-H_3PO_4 was compared with other adsorbents reported in the literature (**Table 5**). The fabricated activated carbon demonstrated the highest ceftriaxone removal efficiency (97.8%), even at a high initial concentration of 200 mg/L. Comparable efficiencies were observed for activated carbon modified with magnetic Fe_3O_4 nanoparticles (97.18%) and a chitosan/graphene oxide nanocomposite functionalized with zirconium (97.1%). While these values were similar, AC-FPAA-H_3PO_4 still exhibited superior performance. Other adsorbents showed significantly lower removal efficiencies: graphene oxide from corn cob (47%), Pseudomonas pudica biomass (50%), Saccharomyces cerevisiae biomass (78%), agricultural waste-derived activated carbon (84%), nano-titanium oxide/chitosan/nano-bentonite composite (93.5%), and unmodified graphene oxide (95.87%). The enhanced adsorption capability of AC-FPAA-H_3PO_4 is likely due to its exceptionally high specific surface area (1895.646 m^2/g), providing

abundant active sites and allowing accommodation of more ceftriaxone molecules. Thus, AC-FPAA-H_3PO_4 ranks among the most effective adsorbents for ceftriaxone removal from aqueous solutions. However, post synthesis surface modifications such as amination or magnetic functionalization can be employed to improve biding and reusability. The proposed techniques may also allow the adsorbent to meet specific environmental remediation needs.

Table 5: Summary of comparison of removal efficiency of ceftriaxone using AC-FPAA-H_3PO_4 with other adsorbents.

Adsorbent	pH	Adsorbate concentration	Kinetic	RE (%)	Reference
AC-FPAA-H_3PO_4	2	200 mg/L	PSO	97.8%	This study
Saccharomyces cerevisiae	6	10 mg/L	PSO	78%	[55]
Graphene oxide	8	25 mg/L	-	95.87%	[56]
Graphene oxide from corn cob	4	14 mg/L	-	47%	[42]
Activated carbon with magnetic Fe_3O_4 nanoparticle composite	3	10 mg/L	PSO	97.18%	[37]
Chitosan/graphene oxide nanocomposite functionalized with zirconium	7.5	20 mg/L	PSO	97.1%	[57]
Pseudomonas pudica biomass	7	50 mg/L	-	50%	[58]
Activated carbon derived from agriculture products waste	7	1.77×10^{-3} mol/L	PSO	84 %	[9]
Assembled composite of nanotitanium oxide/chitosan/nano-bentonite	5	-	PSO	93.5 %	[59]

4. Conclusion

This study successfully synthesized micro-mesoporous activated carbon (AC-FPAA-H_3PO_4) from *A. angustifolium* fruit shells via H_3PO_4 activation (4 M, 600°C, 1 h) for ceftriaxone removal. The activated carbon showed a high surface area (1895.646 $m^2\ g^{-1}$) with the removal efficiency of 97.8% at pH 2, 200 mg/L initial concentration, and 298.15 K within 1 hour. The adsorption process followed both Langmuir (monolayer, R^2=0.9862) and Freundlich (multilayer, R^2=0.9833) isotherms, with kinetics best described by pseudo-second-order (R^2=0.982) and intraparticle diffusion (R^2=0.973) models. Thermodynamics confirmed a spontaneous (ΔG = -6.80 kJ mol^{-1}), exothermic (ΔH = -4.43 kJ mol^{-1}), and entropy-driven (ΔS = 7.69 J $mol^{-1}\ K^{-1}$) process. AC-FPAA-

H_3PO_4 demonstrated high efficacy in real water matrices (98.61% river water; 97.15% well water) and maintained significant removal after five cycles without the regeneration of active sites (65.04% synthetic, 88.05% river, 90.44% well water). This novel, reusable adsorbent offers a promising low-cost solution for organic contaminant removal in water treatment.

Acknowledgements:

Funding: The study was funded by the Sokoine University of Agriculture.

Ethical approval: Not applicable

Consent to Participate declaration: not applicable

Consent to Publish declaration: not applicable

Conflict of interest statement: On behalf of all authors, the corresponding author states that there is no conflict of interest.

Author Contribution declaration: All authors have accepted responsibility for the entire content of this manuscript and consented to its submission to the journal, reviewed all the results and approved the final version of the manuscript. B.K. Conceptualization, methodology, formal analysis, investigation, writing original draft preparation. A.M. Conceptualization, methodology, formal analysis, writing original draft preparation. E.L. Investigation, methodology, review and editing.

Supplementary

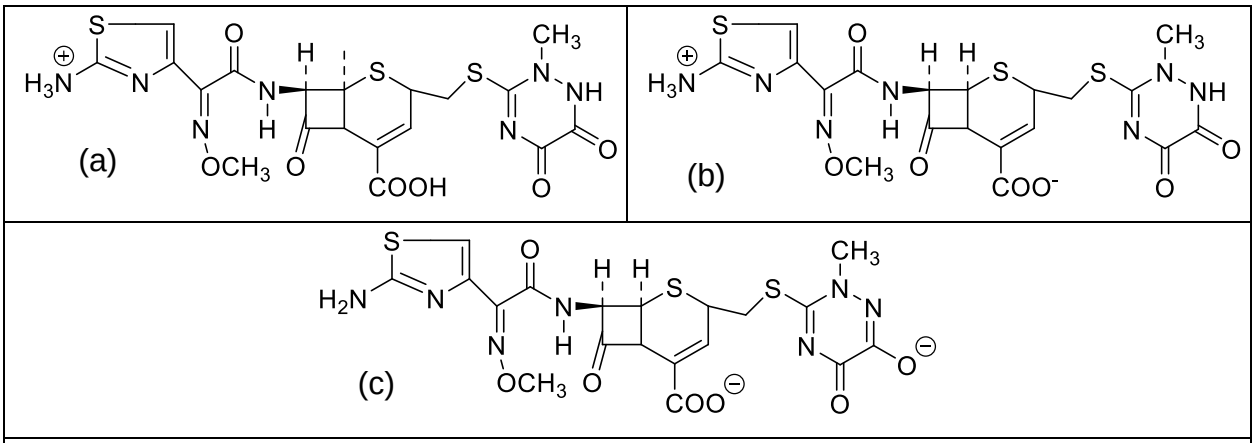

Fig.S1: Proposed chemical speciation of ceftriaxone: (a) ceftriaxone at pH 1 (b) ceftriaxone at pH 2 (c) ceftriaxone at pH above 2.

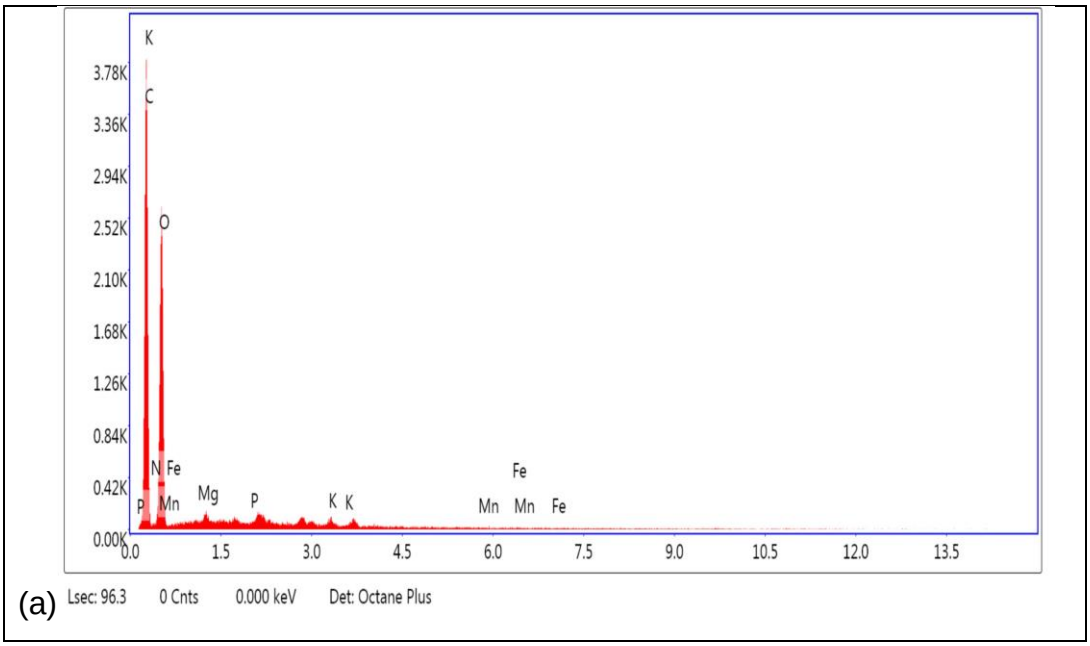

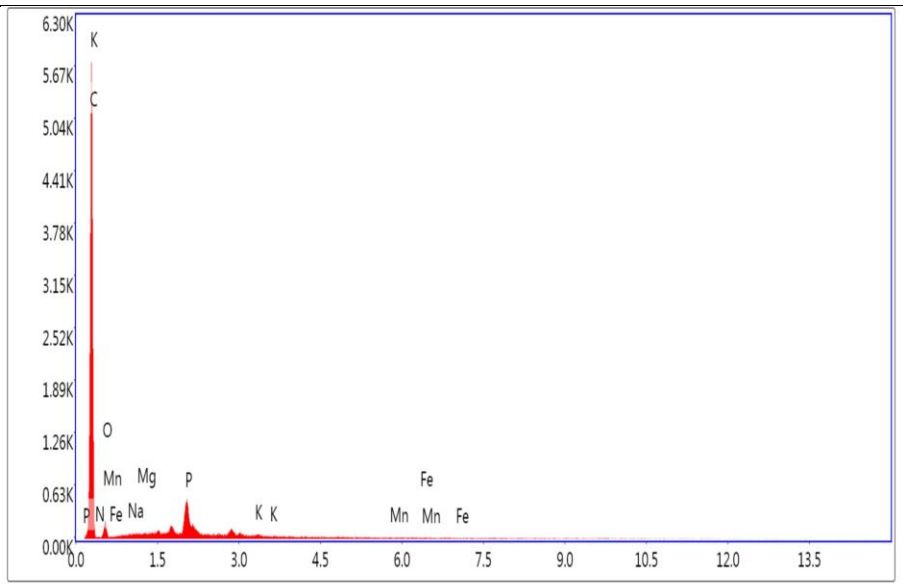

(b)

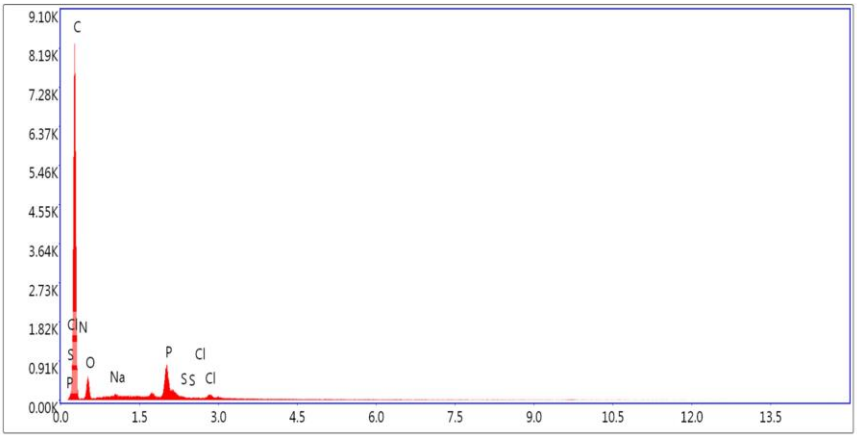

(c)

Fig.S2: EDAX spectrum results. .(a) FPAA (b) AC-FPAA-H_3PO_4 (c) AC-FPAA-H_3PO_4 after adsorption

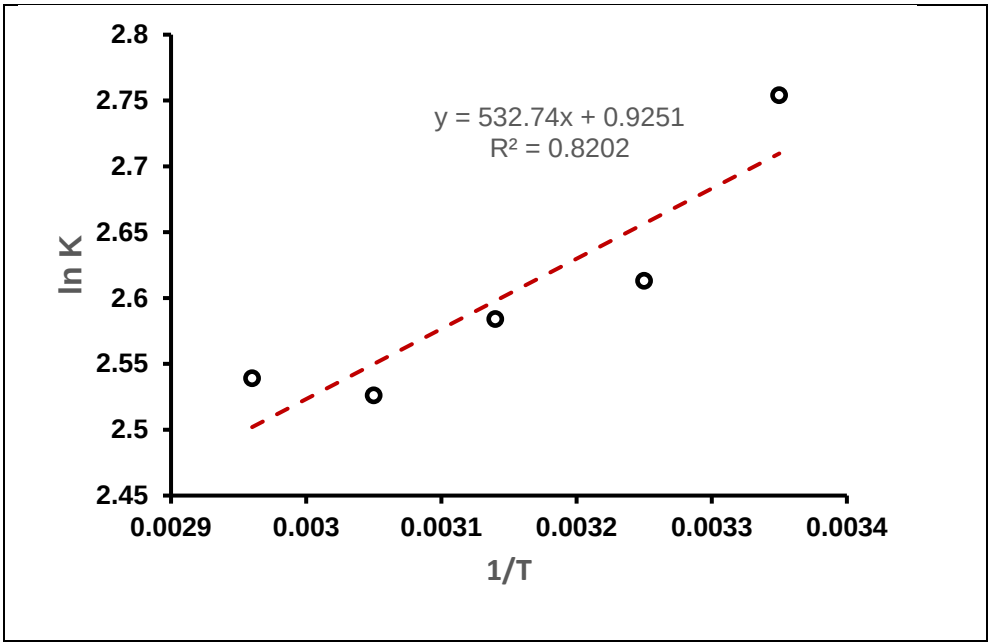

Fig.S3 Thermodynamic study, plot of ln K versus 1/T

Table S1: Comparative summary of FTIR peaks before and after activation of FPAA

Wave number (1/cm) of FPAA	Wave number (1/cm) of AC-FPAA-H3PO4	Bond	Functional group
1029		C-N	Amnine
	1072	P-O-P and P^{+}-O	Phosphate chains
1249	1253	C-O	Ether or carboxylic acids
1379	1381	-CH3	Methyl groups
-	1466,1570	C=C	Aromatic rings
1616	-	C=C	Alkenes
1722	-	C=O	Aldehydes, ketones ,carboxylic acids
2887,2980	2883,2980	C-H	Alkanes
3340	-	O-H	Alcohols, Phenols
3651	3657	Free O-H	Hydroxyl group

Table S2: Summary of parameters of Langmuir and Freundlich isotherms models

Isotherm model	parameters	values
Freundlich	K_F (L/mg)	3.119
	n	1.5225
	R^2	0.9833
Langmuir	q_{max} (mg/L)	72.99
	K_L	0.02937
	R_L	0.145
	R^2	0.9862

Table S3: Summary of adsorption kinetics

Kinetic model	Parameter	Value
Pseudo-first order	Slope	-0.8637
	intercept	2.4241
	q_e^* (mg/g)	435.87
	q_e	265.46
	k_1	1.9891
	R^2	0.9026
Pseudo-second order	Slope	0.0023
	intercept	0.0003
	q_e^* (mg/g)	435.87
	q_e (mg/g)	434.76
	k_2	0.01763
	R^2	0.98241
Elovich	slope	51.014
	intercept	376.76
	α (mg/g min)	0.0196
	β (mg/g)	82184.476
	R^2	0.9054
Weber's model	k_i	190.62
	C_i	195.89
	R^2	0.973

Table S4: Summary of conductivity and pH of real water sample

Water sample	Conductivity	pH
Distilled water (DW)	2.54 µS	7.30
River water (RW)	2.24 mS	8.02
Well water (WW)	11.68 mS	7.58